Azobenzene-containing block copolymers: the interplay of light and morphology enables new functions

Yue Zhao* and Jie He

DOI: 10.1039/b821589h

In azobenzene-containing block copolymers (azo BCPs), the reversible *trans–cis* photoisomerization of the chromophore can be coupled with the microphase separation-induced morphology. Recent studies revealed a number of new functions generated from the interaction of photoactivity and self-organized nanostructures in BCPs. In this paper, we highlight and discuss representative examples that include photoinduced order and patterning of nanostructures in thin films, photosensitive thermoplastic elastomers, BCPs for holographic gratings and photocontrolled morphological transitions in solution.

1. Introduction

Azobenzene-containing polymers (referred to as azo polymers hereafter) and block copolymers (BCPs) represent two active research fields. For the former, the reversible *trans–cis* photoisomerization of azobenzene is the center of interest in exploring light-responsive polymers.[1–5] For the latter, microphase separation-induced morphology and the related self-organized nanostructures both in the solid state[6–9] and in solution[10–12] have attracted much attention. It can be expected that bringing the appealing features of azo polymers and BCPs together could result in interesting systems. In early reports involving azo BCPs,[13–16] azobenzene (rod-shaped in the stable *trans* form) was mainly used as a mesogen for liquid crystalline polymers (LCPs); those azo BCPs were synthesized using anionic polymerization or post-functionalization methods. In recent years, the interest in azo BCPs has been boosted by the accessibility of controlled radical polymerizations such as atom transfer radical polymerization (ATRP)[17] and reversible addition–fragmentation chain transfer polymerization (RAFT).[18] A fast growing number of studies on azo BCPs have been reported by many groups.[19–58] Of particular interest is the exploitation of the interplay between the photoactivity and microphase separated morphology that allows specific new functions to be generated. This often requires rational design of azo BCPs and their ingenious use. By highlighting and discussing some representative examples, this paper aims at sparking more interest for this challenging and exciting issue in the research and development of azo BCPs.

Département de chimie, Université de Sherbrooke, Sherbrooke, Québec, Canada J1K 2R1. E-mail: yue.zhao@usherbrooke.ca; Fax: +1 819 8218017; Tel: +1 819 8217090

2. Photoinduced morphology change, ordering and patterning

The rich variety of self-organized nanostructures of BCPs in the solid state is the

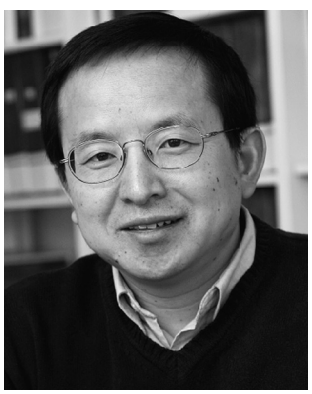

Yue Zhao received his B.S. degree in 1982 from the Chengdu University of Science and Technology in China. He went to France in 1983 and studied at École Supérieure de Physique et de Chimie de Paris with Prof. Lucien Monnerie. After obtaining his PhD in 1987, he did a post-doctoral study with Prof. Robert Prud'homme at Laval University in Canada. In 1991, he joined the Chemistry Department of the University of Sherbrooke and has been a full professor since 2000. His current research focuses on the design, synthesis and study of stimuli-responsive, self-assembled and nanostructured polymer and liquid crystal materials.

Jie He received his BS (2005) and MS degree (2008) from Sichuan University, both in polymer science. He is currently a PhD student in the Laboratory of Polymers and Liquid Crystals under the supervision of Prof. Yue Zhao. His doctoral research focuses on photo-responsive block copolymers in the solid state.

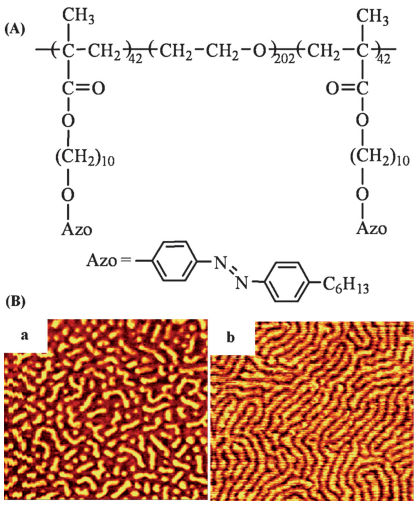

Fig. 1 (A) Chemical structure of the triblock copolymer used for the photoinduced morphology change in a monolayer Langmuir–Blodgett film. (B) AFM topological images (1 μm × 1 μm) showing the morphology of the film on mica with azo groups in the *trans* (a) and *cis* form (b). Adapted with permission from ref. 32.

feature of attraction for much research.[6–9] With azo BCPs, it is conceivable that the *trans–cis* photoisomerization occurring inside the nanostructures may affect the morphology. Kadota *et al.* demonstrated this by using a Langmuir–Blodgett (LB) film of an ABA triblock copolymer (Fig. 1) that has poly(ethylene oxide) (PEO) as the midblock and a polymethacrylate bearing azo side groups as the end blocks.[32] Note that all chemical structures are drawn to show the polymer blocks and their number of monomer units, the end and block linking groups are omitted. The monolayer film on mica with *trans* azo groups displayed a morphology characterized by a mixture of dot- and rod-shaped microdomains of the azo polymer block. In contrast, when the film was prepared with azo groups converted to the *cis* isomer by UV irradiation, the long stripes of the microdomains were observed (Fig. 1). This photoinduced morphology change was attributed to an anisotropic expansion of the microdomains with azo groups in the *cis* form, as the more polar *cis* isomer became in contact with the water surface. The microdomain expansion also resulted in a reduction of the height difference (measured by AFM), from 1.70 ± 0.25 nm for the film with the *trans* isomer to 1.05 ± 0.250 nm for the film with the *cis* isomer. This morphology change was found to be reversible upon slow thermally induced reverse *cis–trans* isomerization.

Achieving long-range order of the self-assembled nanostructures in BCPs is key to enable potential applications.[6–9] The photoinduced orientation of azo groups can be explored for this purpose. Yu *et al.* synthesized a diblock copolymer composed of PEO and a side-chain liquid crystalline polymer (SCLCP) bearing azo mesogens (Fig. 2).[36] In a film, about 100 nm thick, cast from toluene solution on a glass slide, PEO cylindrical nanodomains were aligned perpendicularly to the substrate surface, like in many PEO-based BCPs.[6] After the film was exposed to linearly polarized visible light (488 nm,

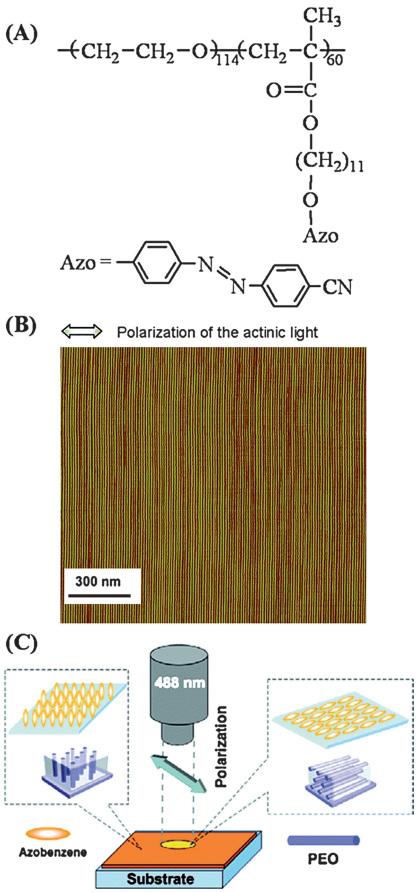

Fig. 2 (A) Chemical structure of the diblock copolymer used for the photoinduced orientation of microphase separated nanocylinders. (B) AFM phase image (1.5 μm × 1.5 μm) showing the uniform orientation induced by linearly polarized irradiation. (C) Schematic illustration showing the orientation of azo groups and PEO nanocylinders in the irradiated and non-irradiated areas. Adapted with permission from ref. 36.

100 mW cm^{-2}) at room temperature and then annealed at 140 °C, PEO nanocylinders were uniformly aligned in-plane and in the same direction as azo groups, *i.e.*, perpendicular to the polarization of the visible light (Fig. 2). The characteristics of the used BCP are important. As it has a smectic-to-isotropic phase transition temperature $T_{si} \approx 158$ °C; the annealing at 140 °C enhances the photoinduced orientation of azo mesogens due to the cooperative motion in the LC phase; and the highly oriented and anisotropic azo polymer matrix imposes the orientation of microphase separated PEO nanocylinders in the same direction as azo mesogens. In principle, uniform ordering of PEO nanocylinders could be obtained in a large area but is mainly determined by the spot size of the irradiation light beam.[36]

Another property of azo polymers that is of great interest is the surface-relief-grating (SRG) that is formed when a thin polymer film is exposed to an interference pattern generated by two coherent laser beams, as a result of the photoisomerization-induced mass transport on the surface.[59,60] Morikawa *et al.* explored the use of SRG to control the organization of PEO nanocylinders based on their film thickness-dependent alignment.[41] They prepared SRG on a thin film of a diblock copolymer composed of PEO and an azo polymethacrylate and showed that at the trough (film thickness ~30 nm) PEO nanocylinders were aligned parallel to the substrate plane (in-plane) while on the crest (film thickness ~70 nm) they were aligned perpendicular to it (out-of-plane). Moreover, similar to the finding of Yu *et al.*,[36] the orientation direction of PEO nanocylinders at the trough could be controlled by the polarization direction of the interference pattern used for the SRG recording. By aligning with azo mesogens, PEO nanocylinders could be oriented either parallel or perpendicular to the edges of the crests.

A follow-up report from the same group showed that the photocontrol over the orientation of nanocylinders could be achieved for polymers other than PEO.[42] Using a diblock copolymer composed of polystyrene (PS) and an azo polymethacrylate (Fig. 3), they showed that vertically aligned PS nanocylinders in a thin film (thickness ~100 nm) prior to irradiation could be brought to parallel

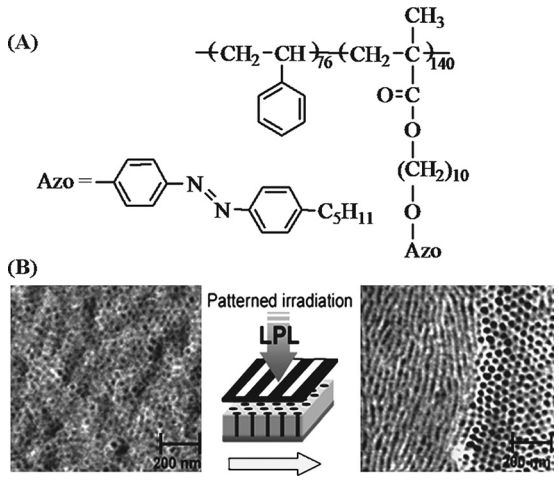

Fig. 3 (A) Chemical structure of the diblock copolymer used for patterned orientational control of nanocylinders by light. (B) AFM phase images of the initial vertical orientation state (left) and the boundary region after patterned exposure to linearly polarized light (right) showing the transition of the orientational state. Adapted with permission from ref. 42.

orientation upon exposure to linearly polarized light. When exposed to non-polarized light, which should erase the orientation of azo mesogens, the initial vertical alignment of PS nanocylinders was recovered. By exposing a film with vertically aligned PS nanocylinders to linearly polarized light through a photomask (10 μm period), alternating regions with PS nanocylinders oriented parallel and perpendicular to the substrate plane could be patterned, with a sharp transition of the orientational state at the interface (Fig. 3). In those reports,[36,41,42] the azo BCPs and the actual irradiation conditions for the photocontrolled orientation of the nanocylinders may differ from each other, but the primary requirement is the same: a thermal annealing step is needed after light illumination to enhance the orientation of azo mesogens while allowing the microphase separation to develop in the oriented matrix. For this reason, the BCP should have an azo SCLCP with an appropriate LC-to-isotropic phase transition temperature, *i.e.*, higher than the T_g or melting temperature of the nanocylinder-forming block. The commanding role of the long-range orientation of azo mesogens in inducing order in BCPs was further confirmed by the observation that by casting a thin film of an azo BCP on rubbed surfaces, nanocylinders of PEO could be uniformly oriented in-plane along the rubbing direction due to the surface-induced orientation of azo mesogens.[37]

3. Photosensitive thermoplastic elastomers

Well before the overwhelming excitement of BCP nanostructures in the context of nanoscience and nanotechnology, the importance of the microphase separation in ABA-type BCPs was recognized, leading to the development of thermoplastic elastomers such as poly(styrene-*b*-butadiene-*b*-styrene) (SBS) and poly (styrene-*b*-isoprene-*b*-styrene) (SIS). In those systems, with a PS content in the range of 20–30 wt%, rubbery polybutadiene (PB) or polyisoprene (PI) chains are interconnected by phase separated PS nanocylinders. At $T < T_g$ of PS, the glassy PS microdomains play the role of physical cross-links that support the elastic deformation (extension of PB or PI chains) under stress.[61] Our group demonstrated that with azo groups incorporated into the structure of a thermoplastic elastomer, interesting functions can be generated as a result of the coupled photoactivity and elasticity.[22,62–65]

The first azo thermoplastic elastomer (ATE) was prepared by grafting an azo polymer onto a SBS triblock copolymer (~30% PS) through radical polymerization of an azo acrylate or methacrylate monomer in solution with dissolved SBS.[62] The resultant ATE, containing about 8% of azo grafts (likely structure in Fig. 4), is transparent and has an excellent elasticity. When its solution-cast films are stretched at room temperature, a long-range molecular orientation of azo groups is obtained along the strain direction. Under strain, this mechanically induced orientation of azo groups can be erased by UV irradiation (*trans–cis* isomerization), but recovered upon subsequent visible light exposure (reverse *cis–trans* isomerization). From the coupled mechanical and optical effects, a diffraction grating (periodic change in refractive index) can be inscribed on a stretched ATE film by its exposure to UV light through a grating photomask, since oriented *trans* azo groups remain in non-irradiated areas

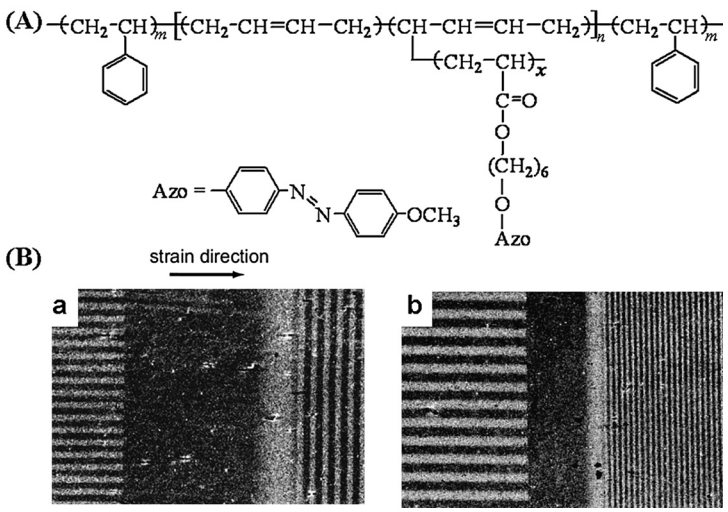

Fig. 4 (A) Chemical structure of the SBS-based triblock copolymer with azo polymer grafts used for mechanically tunable diffraction gratings. (B) Optical micrographs of two gratings (10 μm fringe spacing) recorded on a film under a 300% extension (a) and the gratings on the same film retracted to the half-length (b). Adapted with permission from ref. 63.

while disordered *cis* azo groups are found in irradiated regions. In addition, the photoisomerization in a stretched ATE film could induce a structural rearrangement involving PS nanodomains, giving rise to a stable grating.[62–65] The tunable feature of the gratings recorded on an ATE is shown by the polarizing photomicrographs in Fig. 4. On a film stretched to 300% extension (thickness ~10 μm under strain), two gratings with a 10 μm fringe spacing were recorded with the fringes parallel and perpendicular to the strain direction using photomasks (the irradiated areas appeared dark). When the stretched film was relaxed to its half-length, the fringe spacing of the perpendicular grating decreased, while it increased for the parallel grating. Since the diffraction angle, Θ, is related to the fringe spacing, Λ, through $\Lambda = \lambda/(2\sin\Theta)$, λ being the wavelength of the probe light (633 nm from a He–Ne laser), we showed that it could be reversibly controlled by an elastic deformation.[63] In addition, mechanically tunable diffraction efficiency and diffraction mode (between Raman–Nath and Bragg regimes) could also be achieved using ATE.[65]

We also designed an ATE with azo groups acting inside the physical cross-links (Fig. 5).[22] It is made up with poly(*n*-butyl acrylate) (P*n*BA) as the rubbery middle block and an azo SCLCP as the end blocks forming cylindrical microdomains. Since the physical cross-links are not formed by an amorphous polymer like PS, but by a LC azo polymer, interesting new features could emerge. In particular, as compared to conventional thermoplastic elastomers, such as SBS that basically is elastic at $T_g^{PB} < T < T_g^{PS}$ and becomes thermoplastic at $T > T_g^{PS}$ because softened PS microdomains can no longer sustain the stress, this ATE exhibits an intermediate elastic regime, as illustrated in Fig. 5. When a film is stretched at $T < T_g$ of the azo polymer, the normal elasticity is observed; the deformation is reversible and no long-range molecular orientation of azo mesogens is induced inside the glassy microdomains upon deformation. However, unlike SBS, the elasticity does not disappear when stretched at $T > T_g$. When stretched at temperatures above T_g but below T_{ni} (nematic-to-isotropic phase transition temperature) of the azo polymer, the LC microdomains can still support part of the elastic extension of the P*n*BA chains, while at the same time, a long-range orientation of azo mesogens is induced inside the deformed LC microdomains. This molecular orientation of azo mesogens can be retained in the relaxed film at room temperature, resulting in a thermoplastic elastomer containing glassy microdomains with oriented azobenzene mesogens. Subsequent deformation from this new azobenzene-oriented state is reversible.

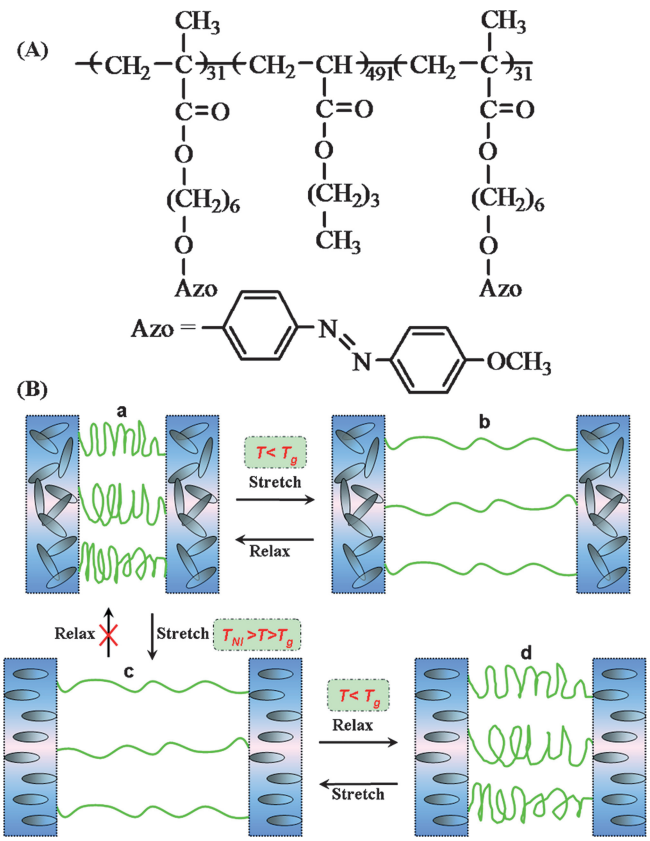

Fig. 5 (A) Chemical structure of the triblock copolymer that is a thermoplastic elastomer with an azo SCLCP forming the physical cross-links. (B) Schematic illustration of the elasticity and the orientational states (only azo groups are shown): (a) initial film before stretching; (b) stretching at $T < T_g$ of the azo polymer (glassy microdomain); (c) stretching at $T_{ni} > T > T_g$ of the azo polymer (liquid crystalline microdomain); and (d) relaxation at $T < T_g$ (glassy microdomain with oriented azo groups). Adapted with permission from ref. 22.

4. Block copolymers for holographic gratings

Azo polymers have long been suggested as a promising material for rewritable holographic data storage.[1–5] However, they suffer from drawbacks limiting the potential for practical applications. One major problem is that high-capacity holographic data storage requires the use of thick samples for volume recording of a large number of gratings, while the high extinction coefficient of azo groups usually means that uniform absorption of photons can only occur in very thin films of azo polymers (hundreds of nanometres in thickness). And with a thin film, the aforementioned SRG due to photoinduced mass transport has also been identified as a handicap for holographic data storage because of the low angular resolution.[33] Schmidt and coworkers addressed those issues by using azo BCPs; their work provides yet another excellent example of ingenious exploitation of photoactivity and morphology.[33,43,44] They proposed the use of BCPs with an amorphous polymer as the majority phase forming the continuous matrix and an azo polymer as the minority phase forming dispersed microdomains. Generally, when an azo polymer in BCPs is confined into microdomains, spheres or cylinders

depending on its volume fraction and interaction with the other polymer, the photoisomerization of azo groups and the related photoorientation or photochemical phase transition can still take place despite the confinement that affects the kinetics or extent of the photoprocesses.[21,40,46] Therefore, with such an azo BCP, while ensuring the photoinduced change in refractive index required for volume holographic recording, thick samples could be used because of the reduced content of azo groups. And with the photoreaction inside dispersed microdomains, the solid matrix could also prevent the formation of undesired SRG.

Their studies demonstrated the potential of this concept. First, it was found that indeed SRG was suppressed in an azo BCP due to the confinement of the azo polymer inside dispersed microdomains.[30] Secondly, thick samples with a low optical density of azo groups could be obtained, not only because of the azo BCP, but there are other possibilities for dilution of azo groups. The azo BCP in Fig. 6 explains the strategy.[43] It has a majority PS block (77.5 wt%) and a minority azo polymer block (22.5%), while the latter is a random copolymer bearing azo groups (8.4%), non-azobenzene mesogens (12.3%) and few residual hydroxyethyl methacrylate groups (1.8%, present due to incomplete functionalization). The use of such a random copolymer for the minority block allows for a decrease of the azo content, knowing that the photoorientation of azo groups could bring the mesogens to orient in the same direction by virtue of the cooperative effect. This was confirmed by the measurement of the maximum index modulation which increased with the content of non-azobenzene mesogens.[33] Moreover, to further reduce the content of azo groups this azo BCP could be blended with a homopolymer of PS.[43] Using a blend composed of 95 wt% of PS and 5 wt% of BCP, in which the azo polymer could form microdomains similar to those in the BCP alone but separated by a larger distance in the continuous PS matrix, thick films of low optical density could be prepared by injection-moulding (the film in Fig. 6B has a thickness of 1.1 mm) and used for multi-angle recording of a large number of stable holographic gratings (Fig. 6C and D); numerous writing and erasing cycles could be performed without degradation of the material.

To hinder the formation of SRG with BCPs, the azo polymer block should be the minority component forming the dispersed phase. If the azo polymer constitutes the continuous phase, photoinduced mass migration cannot be prevented from occurring and SRG can be formed. Here it should be emphasized that SRG is undesired for volume holographic recording, but is of great interest for other photonic applications, for which high diffraction efficiency is a key requirement.[1–5] To this regard, the use of azo BCPs may also be beneficial. Yu *et al.* investigated the formation of SRG on a BCP whose azo polymer is the majority component in volume with respect to the PEO block (Fig.7).[24] A spin-coated thin film (thickness ~600 nm) was pre-irradiated with UV light (366 nm) to achieve a photostationary state rich in *cis* azo groups, then an interference pattern (488 nm) was applied for the recording of a holographic grating (2 μm fringe spacing) at room temperature. Under this condition, azo groups were converted to the *trans* form and oriented in the irradiated (bright) areas, while disordered *cis* azo groups remained in the non-irradiated (dark) areas. In addition to the index grating, a SRG with a small height of surface modulation (16 nm) was also observed. However, after annealing at 100

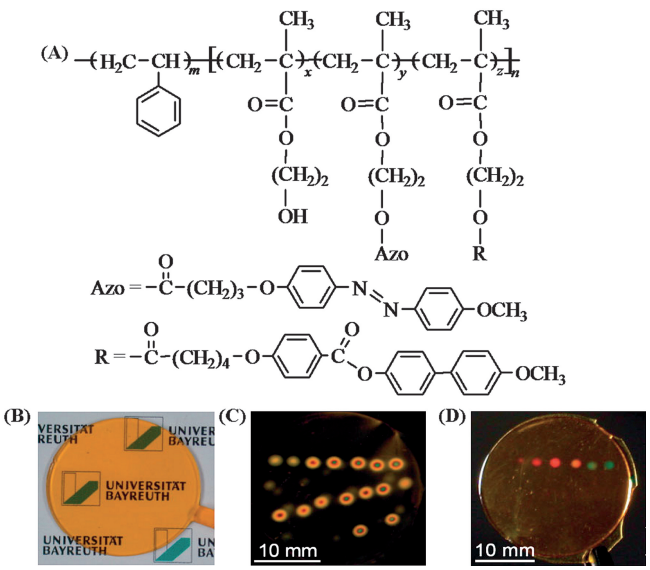

Fig. 6 (A) Chemical structure of the diblock copolymer used for thick samples suitable for volume holographic recording. (B) Picture of a thick film (1.1 mm in thickness) obtained by injection-molding of a blend of the copolymer (5 wt%) with polystyrene (95 wt%). (C) Polarizing photomicrograph showing several holograms recorded in the thick film. (D) Photograph showing the first diffraction order of some holograms under white light illumination. Adapted with permission from ref. 43.

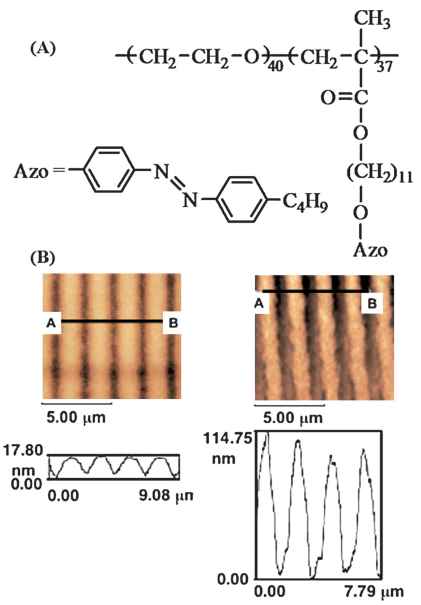

Fig. 7 (A) Chemical structure of the diblock copolymer used for recording enhanced surface-relief-grating on thin films. (B) AFM topological images and surface profiles for a grating before (left) and after (right) annealing in the liquid crystalline phase, showing a drastic increase of the height of surface modulation. Adapted with permission from ref. 24.

°C for 24 h (in the smectic phase), the height of surface modulation increased drastically to 110 nm (Fig. 7), which resulted in an increase in the first-order diffraction efficiency by almost two orders of magnitude. Different microphase separation processes in the irradiated and non-irradiated areas during annealing, with oriented *trans* azo and disordered cis azo groups were believed to have created a pressure gradient leading to an enhanced mass transport on the surface.

5. Photocontrolled morphological transitions in solution

The discussion made so far concerns azo BCPs in the solid state. In solution, if the solvent is block selective, segregation of the blocks can take place and lead to self-assembled nanostructures usually in the form of micellar aggregates such as core–shell micelles and vesicles.[10–12] Likewise, the photoisomerization of azo groups inside the nanostructures may have a consequence. Using azo BCPs, our group demonstrated the first polymer micelles and vesicles that can be reversibly dissociated and reformed upon UV and visible irradiation.[25,26]

The azo BCP is a diblock copolymer whose hydrophilic block is a random copolymer of poly(*tert*-butyl acrylate-co-acrylic acid) and whose hydrophobic block is an azo polymethacrylate (Fig. 8). Its core–shell micelles or vesicles displayed photocontrolled dissociation and formation. In the experiment shown in Fig. 8, when UV light (360 nm) was applied to a solution of vesicles (in dioxane–water), the transmittance of the probe light (633 nm) increased quickly due to the dissociation of vesicles; while once the illumination was switched to visible light (440 nm), the transmittance dropped as a result of the reformation of the aggregates in solution. Scanning electron microscopy (SEM) observations on samples cast from the solution before UV irradiation (marked by A), after 40 s UV irradiation (B) and after 40 s visible irradiation (C) corroborated with the transmittance measurement. The higher and essentially unchanged transmittance was obtained with molecularly dissolved BCP chains (in dioxane) subjected to the same UV and visible light exposure. A photoswitchable polarity of the azo polymer block was found to be at the origin of this photoinduced morphological transition.[26] Upon illumination of the micellar solution with UV light, *trans* azo groups are converted into the cis isomer, which results in a large increase in polarity of the chromophore, from a near zero dipole moment (for the *trans* isomer) to a dipole moment of ~4.4 D for the *cis* isomer. The consequence of this polarity increase is that the azo polymer block is no longer hydrophobic enough to preserve the micellar association and they are dissociated. When visible light is applied to the solution with dissolved BCP chains, azo groups are converted back to the *trans* form and the recovered hydrophilic–hydrophobic balance results in the formation of micelles.

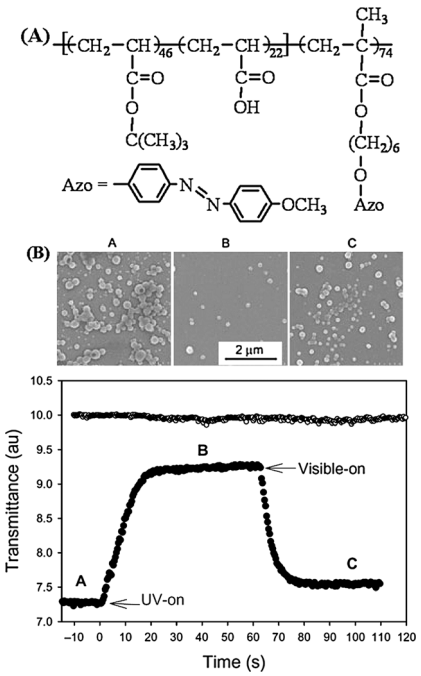

Fig. 8 (A) Chemical structure of the diblock copolymer used for photoinduced morphological transition of micellar aggregates in solution. (B) Changes in the transmittance of a vesicle solution (in dioxane–water) illuminated with UV (360 nm) and then visible light (440 nm), showing the reversible dissociation and formation of micellar aggregates, being corroborated by SEM images recorded on samples cast from the solution before UV, after UV and after subsequent visible light exposure. Adapted with permission from ref. 26.

Other photoinduced morphological transitions of azo BCPs in solution were reported. Han *et al.* showed that an amphiphilic diblock copolymer composed of poly(*N*-isopropylacrylamide) and an azo polymethacrylate could form giant, micrometre-sized vesicles in a mixed solvent of water–tetrahydrofuran, with the hydrophobic azo polymer constituting the membrane of a vesicle.[56] The large size of the aggregates made it possible to observe photoinduced morphological changes directly on an optical microscope. They found that upon UV irradiation, the *trans–cis* isomerization of azo groups led to a 17% increase in the size of the vesicles, while the initial size was recovered upon subsequent visible irradiation. A change in the packing of azo groups or in the solubility of the azo polymer in the solvent could account for the reversible swelling and contraction of the vesicles. On the basis of the same principle of photoinduced polarity change, reversible morphological transitions of micellar aggregates (dissociation and size change) have also been reported for azo "graft-like" copolymers[66] and BCPs containing a switchable chromophore other than azobenzene.[67]

6. Discussion and outlook

The above highlighted works on azo BCPs are good examples of generating specific functions by making use of the interplay of the photoisomerization of azobenzene and the microphase separation induced morphology. Below is a brief discussion in relation to the highlighted systems. However, new functions that remain to be discovered are not limited to those systems.

The use of photoorientation of azo groups to obtain long-range ordering or patterning of the nanostructures in BCPs is worth being pursued. There is a large body of knowledge on the photoorientation of azo polymers,[1–5] which can be exploited to achieve photoinduced ordering or patterning at a more complex level. For instance, in addition to the in-plane (horizontal) and out-of-plane (vertical) orientation of nanocylinders, an oblique orientation with the nanocylinders making an angle to the surface normal could be realized. For this, optically configured oblique orientation of azo mesogens is necessary. It would also be interesting to know what the photoorientation of azo groups can do on other

types of morphology such as lamellar phases.

Regarding thermoplastic elastomers, new triblock copolymers can be designed to have azo groups either on the midblock or on the end blocks. On the one hand, a rubbery azo SCLCP (T_g below room temperature) can be used as the midblock, together with another polymer having a high T_g or T_m (melting temperature) for the end blocks. Thin films of such an ATE can be prepared by solution-casting (unlike conventional elastomers with chemical cross-links) and stretched at room temperature to generate a long-range orientation of azo mesogens. It would be interesting to investigate the effect of photoisomerization (between oriented *trans* and disordered *cis* azo groups) on the elastic force. On the other hand, in addition to mechanically tunable diffraction gratings,[62–65] exploitation for new functions is possible. For instance, by having azo mesogens on the end blocks forming the physical cross-links, the photoisomerization may have a plasticization effect on the rigid microdomains, which could be enhanced if the photoisomerization induces a photochemical LC-to-isotropic phase transition (isotropic state may be more fluid).[3] Since the elastic deformation of thermoplastic elastomers is governed by the rigidity of the microdomains that prevents the relaxation or plastic flow of rubbery chains, this photoinduced effect could be used for photocontrollable plasticity.

With dispersed microdomains of azo polymer in BCPs, the suppression of SRG and the dilution of azo groups make the use of thick samples possible, which holds promise for volume holographic recording.[43,44] But the severe confinement renders the photoinduced orientation of azo groups more difficult (longer holographic writing time).[33] How to obtain fast and stable orientation of azo groups under confinement may be challenging. It would be interesting to investigate the use of supramolecular azo BCPs. If azo groups and mesogens are linked to the minority polymer block through H-bonds, the dynamic nature of the non-covalent association may somehow decouple the orienting side groups from chain backbone and thus increase the rate of photoorientation. The use of azo BCPs for more efficient SRG on thin films is worth a greater effort too.[24] As compared to azo homopolymers or random copolymers, for which the photoisomerization basically induces a change in molecular conformation and/or molecular order, BCPs provide an additional photosensitive variable in play: the morphology. It is of interest to understand how the microphase separation process (kinetics and order) can be coupled to the photoisomerization occurring upon application of an interference pattern and how all this can enhance the mass migration.

In the case of azo BCPs in solution, more possibilities of photocontrolled morphological transitions can be envisioned. For an azo BCP whose micelle can be reversibly dissociated and formed upon UV and visible irradiation, if the micelle core formed by the azo polymer is slightly cross-linked to prevent the dissociation, reversible swelling and contraction of the micelle should be observed. The key requirement for the disruption of micellar aggregates in solution is the difference in polarity between the *trans* and *cis* isomer. It is thus of interest to calculate the change in dipole moment upon the photoisomerization of azobenzene with different substitution patterns. The revealed azo derivatives having the largest polarity change can be used to design azo BCPs for photochangeable morphologies. It is also important to understand the effects of the absolute and the relative block lengths on the photoinduced shift of the hydrophilic–hydrophobic balance. BCP samples with well-defined compositions (same azo polymer block length with different lengths for the hydrophilic block, or *vice versa*) can be used for this end.

Finally, it should be noted that although this paper focuses on azo BCPs, it is conceivable that some discussed functions or properties arising from the interplay of light and BCP morphology could also be obtained by using other photochromic molecules. This is the case with photosensitive thermoplastic elastomers and volume holographic gratings, where what is required is essentially a photoinduced change in the refractive index. Other chromophores whose photoreactions induce a large polarity change can also be employed to design BCP micelles that undergo light-induced morphological transitions.[67,68] However, azobenzene remains the chromophore of choice for the photocontrolled ordering of BCP nanostructures and enhanced SRG, or any desired function or property where an efficient and controllable photoinduced molecular orientation and/or motion is the key condition.

Acknowledgements

Y. Z. is grateful to all the students and collaborators who have made contributions to his group's studies on azo block copolymers, particularly, Dr Li Cui, Mrs Xia Tong, Dr Guang Wang, Dr Shuying Bai and Prof. Tigran Galstian (Laval University). He also acknowledges financial support from the Natural Sciences and Engineering Research Council of Canada (NSERC), le Fonds québécois de la recherche sur la nature et les technologies of Québec (FQRNT), Université de Sherbrooke, St-Jean Photochemicals Inc. (St-Jean-sur-Richelieu, Québec, Canada), the Cancer Research Society Inc. (Canada) and the FQRNT-funded Center for Self-Assembled Chemical Structures (CSACS).

References

1 K. Ichimura, *Chem. Rev.*, 2000, **100**, 1847–1874.
2 A. Natansohn and P. Rochon, *Chem. Rev.*, 2002, **102**, 4139–4175.
3 T. Ikeda, *J. Mater. Chem.*, 2003, **13**, 2037–2057.
4 N. Viswanathan, D. Y. Kim, S. Bian, J. Williams, W. Liu, L. Li, L. Samuelson, J. Kumar and S. K. Tripathy, *J. Mater. Chem.*, 1999, **9**, 1941–1955.
5 *Smart Light-Responsive Materials: Azobenzene-Containing Polymers and Liquid Crystals*, ed. Y. Zhao and T. Ikeda, John Wiley, Hoboken, New Jersey, 2009.
6 E. Huang, L. Rockford, T. P. Russell and C. J. Hawker, *Nature*, 1998, **395**, 757–758.
7 F. S. Bates and G. H. Fredrickson, *Phys. Today*, 1999, **52**, 32–38.
8 C. Park, J. Yoon and E. L. Thomas, *Polymer*, 2003, **44**, 6725–6760.
9 T. P. Lodge, *Macromol. Chem. Phys.*, 2003, **204**, 265–273.
10 D. E. Discher and A. Eisenberg, *Science*, 2002, **297**, 967–973.
11 J. Rodríguez-Hernández, F. Chécot, Y. Gnanou and S. Lecommandoux, *Prog. Polym. Sci.*, 2005, **30**, 691–724.
12 C. J. F. Rijchen, O. Soga, W. E. Hennink and C. F. van-Nostrum, *J. Controlled Release*, 2007, **120**, 131–148.
13 R. Bohnert and H. Finkelmann, *Macromol. Chem. Phys.*, 1994, **195**, 689–700.
14 M. Walther, H. Faulhammer and H. Finkelmann, *Macromol. Chem. Phys.*, 1998, **199**, 223–237.
15 A. Martin, C. Tefehne and W. Gronski, *Macromol. Rapid Commun.*, 1996, **17**, 305–311.

16 G. Mao, J. Wang, S. R. Clingman, C. K. Ober, J. T. Chen and E. L. Thomas, *Macromolecules*, 1997, **30**, 2556–2567.
17 K. Matyjaszewski and J. Xia, *Chem. Rev.*, 2001, **101**, 2921–2990.
18 J. Chiefari, Y. K. Chong, F. Ercole, J. Krstina, J. Jeffery, T. P. T. Le, R. T. A. Mayadunne, G. F. Meijs, C. L. Moad, G. Moad, E. Rizzardo and S. H. Thang, *Macromolecules*, 1998, **31**, 5559–5562.
19 Y. Tian, K. Watanabe, X. Kong, J. Abe and T. Iyoda, *Macromolecules*, 2002, **35**, 3739–3747.
20 L. Cui, Y. Zhao, A. Yavrian and T. Galstian, *Macromolecules*, 2003, **36**, 8246–8252.
21 X. Tong, L. Cui and Y. Zhao, *Macromolecules*, 2004, **37**, 3101–3112.
22 L. Cui, X. Tong, X. Yan, G. Liu and Y. Zhao, *Macromolecules*, 2004, **37**, 7097–7104.
23 H. Yu, A. Shishido, T. Ikeda and T. Iyoda, *Macromol. Rapid Commun.*, 2005, **26**, 1594–1598.
24 H. Yu, K. Okano, A. Shishido, T. Ikeda, K. Kamata, M. Komura and T. Iyoda, *Adv. Mater.*, 2005, **17**, 2184–2188.
25 G. Wang, X. Tong and Y. Zhao, *Macromolecules*, 2004, **37**, 8911.
26 X. Tong, G. Wang, A. Soldera and Y. Zhao, *J. Phys. Chem. B*, 2005, **109**, 20281–20287.
27 Y. K. Han, B. Dufour, W. Wu, T. Kowalewski and K. Matyjaszewski, *Macromolecules*, 2004, **37**, 9355–9365.
28 X. He, H. Zhang, D. Yan and X. Wang, *J. Polym. Sci., Part A: Polym. Chem.*, 2003, **41**, 2854–2864.
29 M. H. Li, P. Keller, J. Yang and P. A. Albouy, *Adv. Mater.*, 2004, **16**, 1922–1925.
30 C. Frenz, A. Fuchs, H. W. Schmidt, U. Theissen and D. Haarer, *Macromol. Chem. Phys.*, 2004, **205**, 1246–1258.
31 L. Cui, S. Dahmane, X. Tong, L. Zhu and Y. Zhao, *Macromolecules*, 2005, **38**, 2076–2084.
32 S. Kadota, K. Aoki, S. Nagano and T. Seki, *J. Am. Chem. Soc.*, 2005, **127**, 8266–8267.
33 M. Häckel, L. Kador, D. Kropp, C. Frenz and H. W. Schmidt, *Adv. Funct. Mater.*, 2005, **15**, 1722–1727.
34 P. Ravi, S. L. Sin, L. H. Gan, Y. Y. Gan, K. C. Tam, X. L. Xia and X. Hu, *Polymer*, 2005, **46**, 137–146.
35 S. L. Sin, L. H. Gan, X. Hu, K. C. Tam and Y. Y. Gan, *Macromolecules*, 2005, **38**, 3943–3948.
36 H. Yu, T. Iyoda and T. Ikeda, *J. Am. Chem. Soc.*, 2006, **128**, 11010–11011.
37 H. Yu, J. Li, T. Ikeda and T. Iyoda, *Adv. Mater.*, 2006, **18**, 2213.
38 H. Yu, S. Asaoka, A. Shishido, T. Iyoda and T. Ikeda, *Small*, 2007, **3**, 768–771.
39 H. Yu, A. Shishido, Y. Iyoda and T. Ikeda, *Macromol. Rapid Commun.*, 2007, **28**, 927–931.
40 H. Yu, Y. Naka, A. Shishido and T. Ikeda, *Macromolecules*, 2008, **41**, 7959–7966.
41 Y. Morikawa, S. Nagano, K. Watanabe, K. Kamata, T. Iyoda and T. Seki, *Adv. Mater.*, 2006, **18**, 883–886.
42 Y. Morikawa, T. Kondo, S. Nagano and T. Seki, *Chem. Mater.*, 2007, **19**, 1540–1542.
43 M. Häckel, L. Kador, D. Kropp and H. W. Schmidt, *Adv. Mater.*, 2007, **19**, 227–231.
44 E. J. Kramer and H. W. Schmidt, *Macromolecules*, 2007, **40**, 2100–2108.
45 B. Qi and Y. Zhao, *Langmuir*, 2007, **23**, 5746–5751.
46 Y. Zhao, B. Qi, X. Tong and Y. Zhao, *Macromolecules*, 2008, **41**, 3823–3831.
47 P. Forcen, L. Oriol, C. Sanchez, R. Alcala, S. Hvilsted, K. Jankova and J. Loos, *J. Polym. Sci., Part A: Polym. Chem.*, 2007, **45**, 1899.
48 D. Wang, G. Ye and X. Wang, *Macromol. Rapid Commun.*, 2007, **28**, 2237–2243.
49 W. Deng, P. Albouy, E. Lacaze, P. Keller, X. Wang and M. Li, *Macromolecules*, 2008, **41**, 2459–2466.
50 D. Wang, H. Ren, X. Wang and X. Wang, *Macromolecules*, 2008, **41**, 9382–9388.
51 X. Tang, L. Gao, X. Fan and Q. Zhou, *J. Polym. Sci., Part A: Polym. Chem.*, 2007, **45**, 2225–2234.
52 J. Li, K. Kamata, M. Komura, T. Yamada, H. Yoshida and T. Iyoda, *Macromolecules*, 2007, **40**, 8125–8128.
53 J. Li, K. Kamata, S. Watanabe and T. Iyoda, *Adv. Mater.*, 2007, **19**, 1267–1271.
54 Y. Zhang, Z. Cheng, X. Chen, W. Zhang, J. Wu, J. Zhu and X. Zhu, *Macromolecules*, 2007, **40**, 4809–4817.
55 W. Su, Y. Luo, Q. yan, S. Wu, K. Han, Q. Zhang, Y. Gu and Y. Li, *Macromol. Rapid Commun.*, 2007, **28**, 1251–1256.
56 K. Han, W. Su, M. Zhong, Q. Yan, Y. Luo, Q. Zhang and Y. Li, *Macromol. Rapid Commun.*, 2008, DOI: 10.1002/marc.200800483.
57 L. Ding, H. Mao, J. Xu, J. He, X. Ding and T. P. Russell, *Macromolecules*, 2008, **41**, 1897–1900.
58 L. Ding and T. P. Russell, *Macromolecules*, 2007, **40**, 2267–2270.
59 P. Rochon, E. Batalla and A. Natansohn, *Appl. Phys. Lett.*, 1995, **66**, 136–138.
60 D. Y. Kim, S. K. Tripathy, L. Li and J. Kumar, *Appl. Phys. Lett.*, 1995, **66**, 1166–1168.
61 T. Pakula, K. Saijo, H. Kawai and T. Hashimoto, *Macromolecules*, 1985, **18**, 1294–1302.
62 S. Bai and Y. Zhao, *Macromolecules*, 2001, **34**, 9032–9038.
63 Y. Zhao, S. Bai, D. Dumont and T. Galstian, *Adv. Mater.*, 2002, **14**, 512–514.
64 S. Bai and Y. Zhao, *Macromolecules*, 2002, **35**, 9657–9664.
65 Y. Zhao, S. Bai, K. Asatryan and T. Galstian, *Adv. Funct. Mater.*, 2003, **13**, 781–788.
66 X. Liu and M. Jiang, *Angew. Chem., Int. Ed.*, 2006, **45**, 3846–3850.
67 H. Lee, W. Wu, J. K. Oh, L. Mueller, G. Sherwood, L. Peteanu, T. Kowalewski and K. Matyjaszewski, *Angew. Chem., Int. Ed.*, 2007, **46**, 2453–2457.
68 Y. Zhao, *J. Mater. Chem.*, 2009, DOI: 10.1039/B819968J.